Distribution of path durations in mobile ad-hoc networks – Palm's Theorem to the rescue

Yijie Han[†], Richard J. La[†∗]
Armand M. Makowski[†], and Seungjoon Lee[‡]

[†] *Department of Electrical and Computer Engineering,*
[‡] *Department of Computer Science,*
University of Maryland, College Park

Abstract

We first study the distribution of path duration in multi-hop wireless networks. We show that as the number of hops along a path increases, the path duration distribution can be accurately approximated by an exponential distribution under a set of mild conditions, even when the link duration distributions are not identical. Then, we develop an approximate model for computing the distribution of link duration under a Random Waypoint (RWP) mobility model, and demonstrate that the path duration distribution converges to an exponential distribution with increasing number of hops. Simulation results obtained using ns-2 simulator are provided to validate our analysis.

Key words: Mobile Ad-Hoc Network, Distributional Convergence, Mobility.

1 Introduction

Routing protocols for multi-hop wireless ad-hoc networks are classified as being either table-driven or on-demand. Table-driven routing protocols attempt to maintain a path between any two nodes at all times, whereas on-demand routing protocols establish a path between two nodes only upon request. Due to node mobility, links along provided paths may become unavailable in an unpredictable manner, a situation which triggers path recovery. These statistical fluctuations of link and path

[1] $\ast$ - corresponding author: hyongla@isr.umd.edu, A. V. Williams Building, Department of Electrical and Computer Engineering, University of Maryland, College Park, MD 20742. Phone: (301) 405-4914. Fax: (301) 314-9281

durations are expected to shape the performance and overheads of on-demand routing protocols. A better and more thorough understanding of these statistical characteristics is therefore warranted. In particular, accurate modeling of link and path durations can help better evaluate the performance of current and new on-demand routing protocols without having to run time-consuming detailed simulations.

The distributions of interest are expected to depend on the mobility models used in the simulations as well as on the range of node speeds. Sadagopan et al. [16] have recently presented a numerical study of the distribution of multi-hop path durations under various mobility models. Their study shows that the distribution of path duration can be accurately approximated by an *exponential* distribution when the number of hops is larger than 3 or 4 for all mobility models considered. However, no *explanation* was offered for the emergence of the exponential distribution.

In this paper, we develop an approximate framework for handling this issue. We show that, under certain conditions, the distribution of path duration (appropriately scaled) converges to an exponential distribution, when the number of hops becomes large. This result is in line with the simulation results provided in [16], and is simply another incarnation of Palm's Theorem [9, Thm. 5-14, p. 157], the one-dimensional precursor of the celebrated Palm-Khintchine Theorem [9, Thm. 5-15, p. 160] – This result states that the superposition of a large number of independent equilibrium renewal processes, each with a small intensity, behaves asymptotically like a Poisson process. A preliminary version of this work was reported in the conference paper [7]. We validate our results through an approximate model which we develop for computing the distribution of link and path durations with varying number of hops under a Random Waypoint (RWP) mobility model. Ns-2 simulation results are provided to further validate our analysis.

The paper is organized as follows. In Section 2 we describe a basic framework for studying the distribution of path durations. Section 3 introduces the version of Palm's Theorem to be used here. This is followed by a discussion of basic modeling assumptions in Section 4. We outline the RWP mobility model in Section 5 and describe how the distributions of link and path durations in the RWP mobility model can be computed in Section 7. Numerical examples are provided in Section 8 under the RWP mobility model. Section 9 provides a justification for the assumptions made in Section 4.

A word on the notation and convention used throughout: We find it convenient to define all the random variables (rvs) of interest on some common probability space $(\Omega, \mathcal{F}, \mathbf{P})$. Two $\mathbb{R}$–valued rvs X and Y are said to be *equal in law* if they have the same distribution, a fact we denote by $X =_{st} Y$. For any $\alpha > 0$, we denote by $\mathcal{E}_\alpha$ any rv that is exponentially distributed with parameter α, i.e.,

$$\mathbf{P}\left[\mathcal{E}_\alpha \le x\right] = \begin{cases} 1 - e^{-\alpha x} & \text{if } x > 0 \\ 0 & \text{if } x \le 0. \end{cases} \quad (1)$$

If H is a probability distribution on $\mathbb{R}_+$, let $m(H)$ denote its first moment which is always assumed to be finite. Convergence in distribution (with n going to infinity) is denoted by $\Longrightarrow_n$. For any $\boldsymbol{x}$ in $\mathbb{R}^2$, with components (η, ζ), set $||\mathbf{x}|| = \sqrt{\eta^2 + \zeta^2}$. Also, with $a > 0$ and $\boldsymbol{x}$ in $\mathbb{R}^2$, let $\mathbb{D}_a(\boldsymbol{x})$ denote the open disk of radius a centered at $\boldsymbol{x}$.

2 A Basic Framework

Consider a mobile ad-hoc network where a set of nodes creates and maintains network connectivity. The routing algorithm is assumed to be an on-demand algorithm, i.e., a path between a source (node) and a destination (node) is set up only when a request is made. A detailed discussion of available on-demand routing protocols is outside the scope of this paper, and we refer the interested reader to the monographs [13,17] for additional information concerning these routing protocols.

Let $V = \{1, \ldots, I\}$ denote the set of I mobile communicating nodes. Each node moves across a domain $\mathbb{D}$ of $\mathbb{R}^2$ or $\mathbb{R}^3$ according to some mobility model. Since there is no fixed infrastructure and nodes are mobile, links between nodes are set up and torn down dynamically. We assume that a link is either up or down. Two nodes without a link between them will establish such a link as soon as they become aware of each other, e.g., when they come within transmission range of each other or when the signal-to-interference-noise-ratio (SINR) at the receiver exceeds a certain threshold, and packets from each other can be successfully decoded. The latter case captures more accurately a physical layer with channel fading. Although this is not needed for the analysis, *communication* links are assumed bidirectional since such bidirectional communication is typically required between two nodes for reliably forwarding packets, e.g., by means of acknowledgments for each transmission.

The establishment of a path from a source node to a destination node requires the *simultaneous* availability of a number of communication links that are *all* up, one originating at the source node and another ending at the destination node – Together these links provide the desired connectivity between source and destination. The *path duration* is then defined as the amount of time that elapses from the moment the path is established until that time when one of the links along the path goes down, due to either mobility or degradation in SINR. For simplicity of analysis, path setup delays are assumed negligible.

We model this situation as follows: For distinct nodes i and j in V, we introduce a $\{0, 1\}$-valued *reachability* process $\{\xi_{ij}(t),\ t \geq 0\}$ with the interpretation that $\xi_{ij}(t) = 1$ (resp. $\xi_{ij}(t) = 0$) if the "link" (i, j) is up (resp. down) at time $t \geq 0$. Such a link (i, j) is understood as a unidirectional link from node i to node j. Since the communication links are assumed bidirectional, we must have $\xi_{ij}(t) = \xi_{ji}(t)$. The process $\{\xi_{ij}(t),\ t \geq 0\}$ is simply an alternating on-off process, with successive up and down time durations given by the rvs $\{U_{ij}(k), k = 1, 2, \ldots\}$ and $\{D_{ij}(k), k = 1, 2, \ldots\}$, respectively.

The reachability processes can be defined in a number of ways. For example, consider the situation where the I nodes travel through the region $\mathbb{D}$. For each i in V, let $\{\boldsymbol{X}_i(t),\ t \geq 0\}$ describe the trajectory of node i, i.e., $\boldsymbol{X}_i(t)$ denotes the position of node i at time $t \geq 0$. If we do not explicitly model channel fading between nodes, it is reasonable to assume that two nodes can communicate with each other reliably if the distance between them is smaller than some fixed transmission range $r_{min} > 0$. Hence, a link between two distinct nodes i and j in V exists at time $t \geq 0$ if and only if their distance is smaller than r_{min}, leading to the definition

$$\xi_{ij}(t) := \mathbf{1}\left[||\boldsymbol{X}_i(t) - \boldsymbol{X}_j(t)|| \leq r_{min}\right], \quad t \geq 0. \tag{2}$$

In the literature this model is known as the disk model [6,14].

Alternative models can take into account the physical layer characteristics of the channel. For instance, two nodes i and j in V can maintain a link between them at time $t \geq 0$ if and only if

$$\min\left(\frac{P_j \cdot F_{ji}(t)}{\Psi_i(t)}, \frac{P_i \cdot F_{ij}(t)}{\Psi_j(t)}\right) > \Gamma \tag{3}$$

for some threshold $\Gamma > 0$, where P_i is the maximum transmission power of node i, and $\boldsymbol{F}(t) = (F_{ij}(t))$ denotes the channel gain matrix (including fading) at time t with $F_{ji}(t) \geq 0$ and $F_{ii}(t) = 0$, $i, j = 1, \ldots I$. Different choices of $\Psi_i(t)$ in (3) lead to different physical layer models. This is discussed in more details in Appendix A.

Next we endow V with a time-varying graph structure by introducing a time-varying set $E(t)$ of directed edges through the relation

$$E(t) := \{(i, j) \in V \times V :\ \xi_{ij}(t) = 1\}, \quad t \geq 0 \tag{4}$$

where by convention we have set $\xi_{ii}(t) = 0$ for each i in V and all $t \geq 0$. Thus, a path can be established (in principle) between nodes s and d at time $t \geq 0$, if node d is reachable from node s by a path in the *undirected* graph derived from the directed graph $(V, E(t))$. Let $\mathcal{P}_{sd}(t)$ denote the set of paths from node s to node d providing this reachability. This set of paths is empty when the nodes s and d are not reachable from each other at time t. When non-empty, this set $\mathcal{P}_{sd}(t)$ may contain more than one path since multiple paths may exist between the pair of nodes s and d. In such a case, the routing protocol in use selects one of the possible paths and let $\mathcal{L}_{sd}(t)$ denote the set of links in $\mathcal{P}_{sd}(t)$ which determines the selected path.

For each link ℓ in $\mathcal{L}_{sd}(t)$, let $T_\ell(t)$ denote the time-to-live or excess life after time t, i.e., $T_\ell(t)$ is the amount of the time that elapses from time t onward until link ℓ

is down. The time-to-live or duration $Z_{sd}(t)$ of the established path from node s to node d using the links in $\mathcal{L}_{sd}(t)$ is defined as the amount of time that elapses from time t until one of the links in $\mathcal{L}_{sd}(t)$ goes down. This quantity is simply given by

$$Z_{sd}(t) := \min\left(T_\ell(t) : \ell \in \mathcal{L}_{sd}(t)\right), \quad t \geq 0. \tag{5}$$

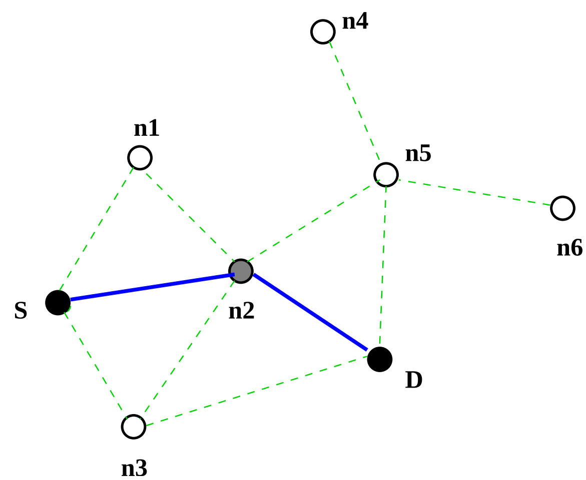

Fig. 1. An example of a path and reachability.

We illustrate these notions on the eight node situation depicted in Fig. 1: Assume that a path is requested from node s to node d at some time $t \geq 0$. A dotted line between two nodes i and j indicates that the bidirectional link between them is up, i.e., $\xi_{ij}(t) = \xi_{ji}(t) = 1$. Here, since there is no dotted line between s and d, i.e., $\xi_{sd}(t) = 0$, no one-hop path can be established at the time of path request. Similarly, we note that $\xi_{n1n4}(t) = 0$ since there is no bidirectional link between nodes $n1$ and $n4$, but $\xi_{n4n5}(t) = 1$ since a bidirectional link exists between nodes n_4 and n_5. However, more than one path can be established from s to d since $\mathcal{P}_{sd}(t)$ comprises the two paths $\{(s, n2), (n2, d)\}$ and $\{(s, n3), (n3, d)\}$. The underlying routing algorithm selects one of them, say $\{(s, n2), (n2, d)\}$, a fact indicated by the bold lines, whence $\mathcal{L}_{sd}(t) = \{(s, n2), (n2, d)\}$. As shown in Fig. 2, the path duration is given by $\min\left(T_{(s,n2)}(t),\ T_{(n2,d)}(t)\right)$, and the excess life of link $(n2, d)$ being smaller than that of link $(s, n2)$, the path duration is therefore given by $T_{(n2,d)}(t)$.

3 Palm's Theorem

We begin our discussion by introducing Palm's Theorem [9]: Let $\{X_\ell^{(n)},\ \ell = 1, \ldots, h^{(n)};\ n = 1, 2, \ldots\}$ be an array of independent $\mathbb{R}_+$-valued rvs with $\{h^{(n)},\ n = 1, 2, \ldots\}$ a monotone increasing sequence of (non-random) integers which exhausts $\mathbb{N}$, i.e., $\lim_{n\to\infty} h^{(n)} = \infty$. Fix $n = 1, 2, \ldots$. For each $\ell = 1, \ldots, h^{(n)}$, the rv $X_\ell^{(n)}$ is distributed according to the cumulative distribution function (CDF) $F_\ell^{(n)}$ given by

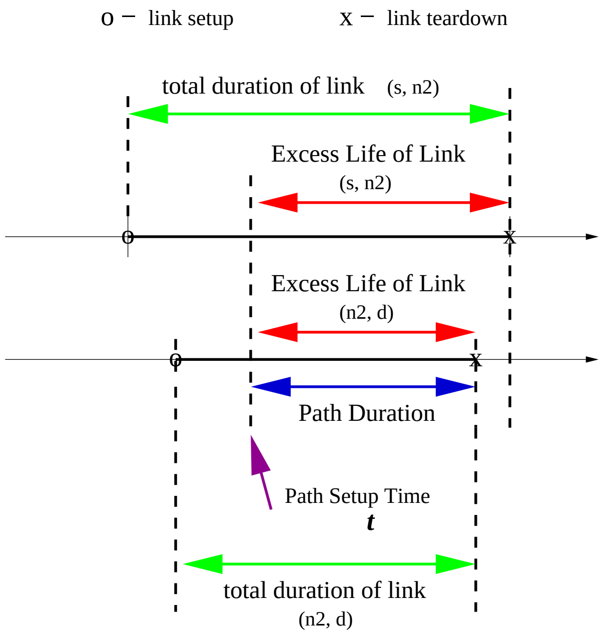

Fig. 2. Link excess life and path duration.

$$F_\ell^{(n)}(x) = \begin{cases} \frac{1}{m(G_\ell^{(n)})} \int_0^x (1 - G_\ell^{(n)}(y))\, dy & \text{if } x > 0 \\ 0 & \text{if } x \leq 0 \end{cases} \tag{6}$$

where $G_\ell^{(n)}$ is a CDF with support in $\mathbb{R}_+$. The distributions $\{G_\ell^{(n)},\ \ell = 1, \ldots, h^{(n)}\}$ are not necessarily identical.

To state the requisite assumptions, we introduce the quantities

$$\lambda_\ell^{(n)} := \left(m(G_\ell^{(n)}) \right)^{-1}, \quad \ell = 1, \ldots, h^{(n)},\ n = 1, 2, \ldots .$$

We assume that the following conditions hold:

Assumption 1 *There exists* $\lambda > 0$ *such that*

$$\lim_{n \to \infty} \sum_{\ell=1}^{h^{(n)}} \lambda_\ell^{(n)} = \lambda\ .$$

Assumption 2 *For every* $x \geq 0$,

$$\lim_{n \to \infty} \left(\max_{\ell = 1, \ldots, h^{(n)}} G_\ell^{(n)}(x) \right) = 0\ .$$

A more concrete way to express Assumption 2 is as follows: For every $x \geq 0$ and any given $\varepsilon > 0$, there exists an integer $n^\star = n^\star(x;\varepsilon)$ such that

$$\max_{\ell=1,\ldots,h^{(n)}} G_\ell^{(n)}(x) \leq \varepsilon, \quad n = n^\star, n^\star + 1, \ldots$$

We can now state Palm's Theorem [9, p. 157] in a form convenient for our purposes.

Theorem 1 *Under Assumptions 1 and 2, it holds that*

$$\min\left(X_\ell^{(n)},\ \ell = 1,\ldots,h^{(n)}\right) \Longrightarrow_n \mathcal{E}_\lambda\ . \tag{7}$$

In other words,

$$\lim_{n\to\infty} \mathbf{P}\left[\min\left(X_\ell^{(n)},\ \ell = 1,\ldots,h^{(n)}\right) \leq x\right] = \begin{cases} 1 - e^{-\lambda x} & \text{if } x > 0 \\ 0 & \text{if } x \leq 0 \end{cases}\ .$$

The so-called homogeneous case assumes the existence of independent and identically distributed (i.i.d.) rvs $\{X_k,\ k = 1,2,\ldots\}$ distributed according to some distribution F given by (6) with another distribution G on $\mathbb{R}_+$, and takes

$$X_\ell^{(n)} = h^{(n)} \cdot X_\ell, \quad \ell = 1,\ldots,h^{(n)}$$

for each $n = 1,2,\ldots$, with corresponding distributions

$$G_\ell^{(n)}(x) = G\left(\frac{x}{h^{(n)}}\right), \quad x \geq 0,\ \ell = 1,\ldots,h^{(n)}\ .$$

Assumption 2 now reads $\lim_{n\to\infty} G_\ell^{(n)}(x) = G(0) = 0$, i.e., a link duration is strictly positive with probability one. The convergence (7) reads

$$h^{(n)} \cdot \min\left(X_\ell\ ;\ \ell = 1,\ldots,h^{(n)}\right) \Longrightarrow_n \mathcal{E}_\lambda$$

where $\lambda = m(G)^{-1}$. Assumption 1 is automatically satisfied since $(m(G_\ell^{(n)}))^{-1} = \frac{\lambda}{h^{(n)}}$ for each $\ell = 1,\ldots,h^{(n)}$.

4 Modeling Assumptions and Distributional Convergence

As discussed in Section 1, the overall performance of an on-demand routing protocol is affected significantly by the overhead it incurs, which in turn depends on the distribution of path durations. Hence, there is a great deal of interest in understanding the distributional properties of the rvs defined through (5).

4.1 The set-up

We are concerned with asymptotic distributional results (as the number of hops becomes large) in the context of the following standard parametric scenario: For each $n = 1, 2, \ldots$, let $V^{(n)} = \{1, \ldots, I^{(n)}\}$ and $\mathbb{D}^{(n)}$ denote the set of mobile nodes and the domain across which the nodes move, respectively. For each node i in $V^{(n)}$, the $\mathbb{D}^{(n)}$-valued process $\{\boldsymbol{X}_i^{(n)}(t),\ t \geq 0\}$ denotes the trajectory of node i in $\mathbb{D}^{(n)}$. The $I^{(n)}$ trajectory processes $\{\boldsymbol{X}_i^{(n)}(t),\ t \geq 0\}$, $i = 1, \ldots, I^{(n)}$, are assumed to be *mutually independent*. Moreover, the stochastic process that governs the arrival of path requests is assumed to be independent of these reachability processes.

Scaling – The situation of interest will be the one where

$$I^{(n)} \sim nI^{(1)} \quad \text{and} \quad \text{Area}(\mathbb{D}^{(n)}) \sim n \cdot \text{Area}(\mathbb{D}^{(1)}) \tag{8}$$

as n goes to infinity; [2] it is customary to reparametrize so that $I^{(n)} = n$. When in force, the scaling (8) guarantees

$$\frac{I^{(n)}}{Area(\mathbb{D}^{(n)})} \sim \frac{I^{(1)}}{Area(\mathbb{D}^{(1)})}, \tag{9}$$

so that the density of nodes, i.e., the number of nodes per unit area, is asymptotically constant.

Stationarity – As the system is expected to run for a long time, we can assume that steady state has been reached. This possibility is captured by taking the $\frac{I^{(n)} \times (I^{(n)}-1)}{2}$ reachability processes to be *jointly stationary*. For distinct $i < j$ in $V^{(n)}$, let the rvs $\{(U_{ij}^{(n)}(k), D_{ij}^{(n)}(k)),\ k = 2, 3, \ldots\}$ denote the sequence of up and down times for the reachability process $\{\xi_{ij}^{(n)}(t),\ t \geq 0\}$. Writing

$$\boldsymbol{W}^{(n)}(k) = ((U_{ij}^{(n)}(k), D_{ij}^{(n)}(k)),\ i < j,\ i, j \in V^{(n)}), \quad k = 1, 2, \ldots,$$

we require that the sequence of rvs $\{\boldsymbol{W}^{(n)}(k),\ k = 2, 3, \ldots\}$ be *strictly stationary*. In particular, for distinct $i < j$ in $V^{(n)}$, the sequence $\{(U_{ij}^{(n)}(k), D_{ij}^{(n)}(k)),\ k = 2, 3, \ldots\}$ constitutes a stationary sequence with generic marginals $(U_{ij}^{(n)}, D_{ij}^{(n)})$. We denote by $G_{ij}^{(n)}$ the CDF of $U_{ij}^{(n)}$. This model is general enough that link dynamics

[2] From now on we omit this qualifier in all asymptotic equivalences.

due to both mobility and channel fading can be captured by appropriately selecting the CDFs for $U_{ij}^{(n)}$.

Well-known results for renewal processes and independent on-off processes in equilibrium [9, Sections 5-6] can be generalized as follows: With $\ell = (i,j)$, in the notation introduced in Section 2, we have

$$\mathbf{P}\left[T_\ell^{(n)}(0) \le x \middle| \xi_{ij}^{(n)}(0) = 1\right] = F_\ell^{(n)}(x), \quad x \in \mathbb{R} \tag{10}$$

where the CDF $F_\ell^{(n)}$ is of the form (6) for some link duration CDF $G_\ell^{(n)}$. In other words, $F_\ell^{(n)}$ is simply the distribution of the forward recurrence time associated with $U_\ell^{(n)}$. From (6) the duration of an one-hop path has a non-increasing probability density function (PDF). If $X_\ell^{(n)}$ denotes any $\mathbb{R}_+$-valued rv distributed according to $F_\ell^{(n)}$, then the relation (10) simply states, with a little abuse of notation, that

$$\left[T_\ell^{(n)}(0) \le x \middle| \xi_{ij}^{(n)}(0) = 1\right] =_{st} X_\ell^{(n)}.$$

The rv (5) can now be viewed as the rv $Z^{(n)}$ defined by

$$Z^{(n)} := \min\left(X_\ell^{(n)} : \ \ell = 1, \ldots, H^{(n)}\right) \tag{11}$$

where $H^{(n)} = |\mathcal{L}_{sd}^{(n)}(0)|$. Due to the underlying stationarity assumptions, it clearly suffices to consider only the case $t = 0$ as we do from now on.

4.2 Modeling assumptions

The form of either (5) or (11) already highlights the sources of difficulty in modeling and studying the distribution of path durations: First, the set $\mathcal{L}_{sd}(0)$ of active links is a *random* subset of $E(0)$, which is determined by the reachability processes (and of the appropriate time-to-live rvs entering (5)). Second, the reachability processes are usually *not* independent of each other, as should be apparent from either formulation (2) or (3). At first blush this seems to preclude applying Palm's Theorem in order to obtain the asymptotic properties of the rv defined at (11). Therefore, in order to make progress, we shall need to make several simplifying assumptions.

Asymptotics of the random set $\mathcal{L}_{sd}^{(n)}(0)$ – Under scaling (8) the average number of hops in a path between two randomly selected nodes typically increases with n. For example, under the disk model (2) with a fixed transmission range, the expected number of hops along a path scales with $\sqrt{n}$. This suggests that we can select a pair of nodes s and d in $V^{(n)}$ such that $\lim_{n\to\infty} |\mathcal{L}_{sd}^{(n)}(0)| = \infty$, where for convenience the sequence $\{|\mathcal{L}_{sd}^{(n)}(0)|,\ n = 1, 2, \ldots\}$ is assumed to be deterministic.

Independence – For each $n = 1, 2, \ldots$, we assume that the reachability processes $\{\xi_{ij}^{(n)}(t),\ t \geq 0\}$ ($i < j$ in $V^{(n)}$) are *mutually independent*. This assumption is not true in general even under the assumption of mutual independence of the trajectory processes. One source of dependence between the reachability processes arises from the fact that two reachability processes $\{\xi_{ij}(t), t \geq 0\}$ and $\{\xi_{jk}(t), t \geq 0\}$ (with distinct i, j, k in $V^{(n)}$) share a common node j, and it is clear that the reachability process $\{\xi_{ik}(t), t \geq 0\}$ is not independent of the first two processes.

A consequence of this independence assumption is that for each $n = 1, 2, \ldots$, the rvs $\{X_\ell^{(n)}, \ell = 1, \ldots, H^{(n)}\}$ are *mutually independent* rvs distributed according to the CDF $F_\ell^{(n)}$ associated by (6) with some link duration CDF $G_\ell^{(n)}$. The CDFs $\{G_\ell^{(n)},\ \ell = 1, \ldots, H^{(n)};\ n = 1, 2, \ldots\}$ are not necessarily identical. We are now ready to discuss the asymptotic behavior of (11) as $H^{(n)}$ becomes large, and the emergence of the exponential distribution in the limit.

4.3 Distributional convergence of a path duration

Assumption 3 *The link duration distributions $\{G_\ell^{(n)},\ \ell = 1, \ldots, H^{(n)}; n = 1, 2, \ldots\}$ satisfy Assumptions 1 and 2 with some constant $\lambda > 0$.*

With obvious identification, we readily obtain from Theorem 1 the following convergence result.

Theorem 2 *Under Assumption 3, we have*

$$\lim_{n\to\infty} \mathbf{P}\left[Z^{(n)} \leq x\right] = \begin{cases} 1 - e^{-\lambda x} & \text{if } x > 0 \\ 0 & \text{if } x \leq 0 \end{cases} . \tag{12}$$

We introduced the assumption of independence of the reachability processes in order to obtain Theorem 2 by an application of Palm's Theorem. While this assumption may be viewed as unrealistic (more on that in a moment), we note that more general versions of Palm's Theorem (or of its variant) are available, and yield similar distributional convergence *without* the independence assumption under a scaling assumption slightly different from Assumption 1 (see [8] for an example). Furthermore, the example using the RWP mobility model in Section 9 suggests that the dependency in link excess lives introduced by the lack of independence of the reachability processes is negligible between two links separated by other intermediate link(s) and is weak even between two neighboring links sharing a common node.

This provides further comfort for the validity of Theorem 2 to the effect that when the number of hops is large (and the link excess lives are approximately independent), the distribution of path duration can be accurately approximated by an exponential rv under a set of mild conditions. As a byproduct, we see that if the path duration can be approximated by an exponential rv, then the inverse of expected value of the path duration is approximately given by the sum of the inverses of expected link durations.

As noted earlier, (6) implies that the PDF of the duration of an one-hop path is a non-increasing function. This observation contrasts with the numerical results (Fig. 6) in [16], where the authors suggest, on the basis of simulation results, that the one-hop path duration may not have a non-increasing PDF. We suspect this might be due to (i) the limited number of statistics they collected from the simulation as a result of low mobility or to (ii) the slightly different definition of path duration used in the paper. Note that the PDF plots become much smoother with increasing mobility or speed of nodes in [16], thereby yielding a larger number of collected samples (e.g., Figs. 6 and 7 vs. Figs. 8 - 10 in [16]).

5 The Random Waypoint Mobility model

The random waypoint (RWP) mobility model without pause [10] is now introduced, It will be used for computing the distributions of link and path durations. Approximations for these quantities are derived in Section 7 when the number of hops grows unbounded.

We begin by describing the model for a single node roaming across a given *convex* domain $\mathbb{D}$ of $\mathbb{R}^2$.[3] The trajectory $\{\boldsymbol{X}(t),\ t \geq 0\}$ of this single node is determined by *linear interpolation* between a sequence of $\mathbb{D}$-valued rvs $\{\tilde{\boldsymbol{X}}_p,\ p = 0, 1, \ldots\}$, the so-called random *waypoints*. For each $p = 0, 1, \ldots$, the node reaches the random waypoint $\tilde{\boldsymbol{X}}_p$ at time T_p, and immediately starts moving on the straight line connecting $\tilde{\boldsymbol{X}}_p$ and $\tilde{\boldsymbol{X}}_{p+1}$ at constant (possibly random) speed $\tilde{S}_p$. With $T_0 = 0$, we see that

$$T_{p+1} = T_p + \frac{\|\tilde{\boldsymbol{X}}_{p+1} - \tilde{\boldsymbol{X}}_p\|}{\tilde{S}_p}. \tag{13}$$

[3] The case where $\mathbb{D}$ is a subset of $\mathbb{R}^3$ can be handled in a similar way. The details are omitted in the interest of brevity.

Moreover, in the interval $[T_p, T_{p+1})$, the position of the node is given by

$$\boldsymbol{X}(t) = \tilde{\boldsymbol{X}}_p + \frac{\tilde{\boldsymbol{X}}_{p+1} - \tilde{\boldsymbol{X}}_p}{\|\tilde{\boldsymbol{X}}_{p+1} - \tilde{\boldsymbol{X}}_p\|} \tilde{S}_p(t - T_p), \quad T_p \le t < T_{p+1} \tag{14}$$

while the instantaneous speed is given by

$$S(t) = \tilde{S}_p, \quad T_p \le t < T_{p+1}. \tag{15}$$

Throughout, we make use of this mobility model under the following standard assumptions: (i) The rvs $\{\tilde{\boldsymbol{X}}_p, \tilde{S}_p,\ p = 0, 1, \ldots\}$ are mutually independent; (ii) The rvs $\{\tilde{\boldsymbol{X}}_p,\ p = 0, 1, \ldots\}$ are i.i.d. rvs which are uniformly distributed over the region $\mathbb{D}$; and (iii) The rvs $\{\tilde{S}_p,\ p = 0, 1, \ldots\}$ are i.i.d. rvs which are uniformly distributed over the finite interval $[S_\star, S^\star]$ with $S_\star > 0$; the limits $S_\star$ and $S^\star$ are the minimum and maximum speed of the node, respectively.

Under these assumptions, it can be shown [11] that a stationary regime exists and $(\boldsymbol{X}(t), S(t)) \Longrightarrow_t (\boldsymbol{X}, S)$ for some $\mathbb{D} \times [S_\star, S^\star]$-valued rv $(\boldsymbol{X}, S)$ with $\boldsymbol{X} = (\eta, \zeta)$. It turns out that the rvs $\boldsymbol{X}$ and S are independent, with the distribution of $\boldsymbol{X}$ independent of the speed distribution used. During the forthcoming discussion, given our interest in this steady state regime, the node's position and its instantaneous speed are always assumed distributed according to the *stationary* version $(\boldsymbol{X}, S)$. Its distributional properties are developed in the remainder of this section.

The CDF of the stationary speed S admits a PDF f_S given by

$$f_S(s) = \frac{1}{s} \cdot \left(\ln \left(\frac{S^\star}{S_\star} \right) \right)^{-1}, \quad S_\star \le s \le S^\star. \tag{16}$$

If we now take $\mathbb{D}$ to be the disk $\mathbb{D}_a(\mathbf{0})$ for some $a > 0$, then the CDF of rv $\boldsymbol{X}$ admits a PDF, denoted hereafter by f_a.[4] By circular symmetry, this PDF depends only on the distance to the origin. To exploit this fact further, we introduce the polar coordinates (R, Θ) of $\boldsymbol{X}$, where R denotes the distance of $\boldsymbol{X}$ to the origin, i.e., $R := \sqrt{\eta^2 + \zeta^2}$, and Θ denotes the angle determined with the η-axis by the line joining the origin to $\boldsymbol{X}$, i.e., $\Theta := \arctan\left(\frac{\zeta}{\eta}\right)$. As argued in [1], the PDF of R is well approximated by the PDF ϕ_a given by

$$\phi_a(r) = \begin{cases} \frac{4r}{a^2}\left(1 - \frac{r^2}{a^2}\right) & \text{if } 0 \le r \le a \\ 0 & \text{otherwise} \end{cases}, \tag{17}$$

[4] Although here we carry out most of the asymptotic analysis of the next section with disks, our results in this section can be extended to the case when a rectangular region is used (see [1] for an example).

while Θ is uniformly distributed on $[0, 2\pi)$. Furthermore, the rvs R and Θ are independent, so that the polar coordinates (R, Θ) of $\boldsymbol{X}$ have a joint PDF which is well approximated by

$$f_{R,\Theta}(r, \theta) = \frac{1}{2\pi}\phi_a(r), \quad 0 \leq r \leq a,\ 0 \leq \theta \leq 2\pi. \tag{18}$$

Noting (see [3, p. 241])

$$f_{R,\Theta}(r, \theta) = f_a(r\cos(\theta), r\sin(\theta)) \cdot r\ , \quad 0 \leq r \leq a,\ 0 \leq \theta \leq 2\pi$$

we conclude to the approximation

$$f_a(\boldsymbol{x}) = \begin{cases} \frac{2}{\pi \cdot a^2}\left(1 - \frac{||\boldsymbol{x}||^2}{a^2}\right) & \text{if } 0 \leq ||\boldsymbol{x}|| \leq a \\ 0 & \text{otherwise} \end{cases}. \tag{19}$$

In particular,

$$f_a(r, 0) = \begin{cases} \frac{2}{\pi \cdot a^2}\left(1 - \frac{r^2}{a^2}\right) & \text{if } 0 \leq r \leq a \\ 0 & \text{otherwise} \end{cases}. \tag{20}$$

The PDF at (20) is plotted in Fig. 3 for different values of a. While the boundary effects preclude the spatial distribution of a node to be uniform on the disk, they diminish with increasing a.

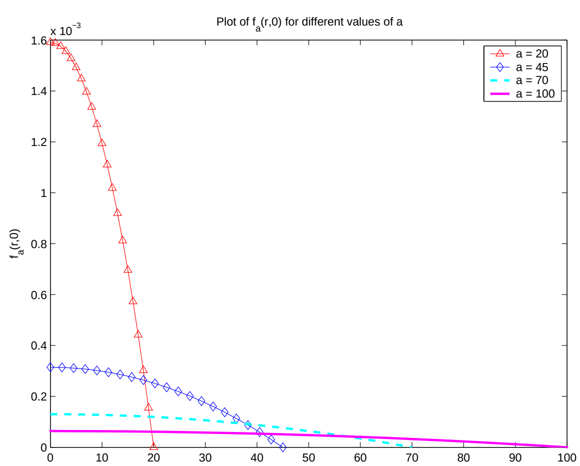

Fig. 3. Plot of $f_a(r, 0)$ for $a = 20, 45, 70, 100$.

6 Asymptotic results for the RWP model

We now return to the parametric scenario of Section 4: For each $n = 1, 2, \ldots$, there are n mobile nodes [5] moving about on the disk $\mathbb{D}_{a_n}(\mathbf{0})$ of radius a_n with $a_n = \alpha\sqrt{n}$ for some $\alpha > 0$. This automatically ensures (8). From now on, we revert back to the notation $\mathbb{D}^{(n)}$ to denote $\mathbb{D}_{a_n}(\mathbf{0})$.

These n nodes move independently of each other, each according to the RWP mobility model over $\mathbb{D}^{(n)}$ as described in Section 5. For each $i = 1, \ldots, n$, let $\boldsymbol{X}_i^{(n)} = (\eta_i^{(n)}, \zeta_i^{(n)})$ denote the (stationary) position of node i. Thus, the rvs $\boldsymbol{X}_1^{(n)}, \ldots, \boldsymbol{X}_n^{(n)}$ are i.i.d. rvs with support on $\mathbb{D}^{(n)}$ whose distributional properties were discussed earlier. In particular, their common PDF f_{a_n} will be approximated by (19). Thereafter we denote by $\boldsymbol{X}^{(n)}$ any $\mathbb{D}^{(n)}$-valued rv distributed according to the distribution with PDF f_{a_n}.

We do not explicitly model the channel fading between nodes and assume that two nodes can communicate with each other reliably if the distance between them is smaller than some transmission range $r_{min} > 0$. This leads to the definition (2) for the reachability processes where the value of r_{min} is fixed and *independent* of n.

For each $\boldsymbol{x}$ in $\mathbb{D}^{(n)}$, we simplify the notation by writing $\mathbb{D}(\boldsymbol{x})$ instead of $\mathbb{D}_{r_{min}}(\boldsymbol{x})$. For any B in $\mathcal{B}(\mathbb{R}^2)$, we have

$$\mathbf{P}\left[\boldsymbol{X}^{(n)} \in B \middle| \boldsymbol{X}^{(n)} \in \mathbb{D}(\boldsymbol{x})\right] = \frac{1}{\mathbf{P}\left[\boldsymbol{X}^{(n)} \in \mathbb{D}(\boldsymbol{x})\right]} \cdot \int_{B(\boldsymbol{x})} f_{a_n}(\boldsymbol{z}) d\boldsymbol{z} \tag{21}$$

where we have set $B(\boldsymbol{x}) := B \cap \mathbb{D}(\boldsymbol{x})$.

The conditional distribution of $\boldsymbol{X}^{(n)}$ given that $\boldsymbol{X}^{(n)}$ lies in the disk $\mathbb{D}(\boldsymbol{x})$ admits a PDF given by

$$f^{(n)}(\boldsymbol{z}|\boldsymbol{x}) = \begin{cases} \frac{f_{a_n}(\boldsymbol{z})}{\mathbf{P}\left[\boldsymbol{X}^{(n)} \in \mathbb{D}(\boldsymbol{x})\right]} & \text{if } \boldsymbol{z} \in \mathbb{D}^{(n)} \cap \mathbb{D}(\boldsymbol{x}) \\ 0 & \text{otherwise} \end{cases} . \tag{22}$$

This conditional distribution has support contained in the disk $\mathbb{D}(\boldsymbol{x})$ with

$$\int_{\mathbb{D}(\boldsymbol{x})} f^{(n)}(\boldsymbol{z}|\boldsymbol{x}) d\boldsymbol{z} = 1,$$

[5] This corresponds to $I^{(n)} = n$.

so that we must have

$$\inf_{\boldsymbol{z}\in\mathbb{D}(\boldsymbol{x})} f^{(n)}(\boldsymbol{z}|\boldsymbol{x})\cdot\pi r_{min}^2 \le 1 \le \sup_{\boldsymbol{z}\in\mathbb{D}(\boldsymbol{x})} f^{(n)}(\boldsymbol{z}|\boldsymbol{x})\cdot\pi r_{min}^2. \tag{23}$$

For each $\boldsymbol{x}$ in $\mathbb{D}^{(n)}$, set

$$M^{(n)}(\boldsymbol{x}) := \sup_{\boldsymbol{z},\boldsymbol{z}'\in\mathbb{D}(\boldsymbol{x})}\left|f^{(n)}(\boldsymbol{z}|\boldsymbol{x}) - f^{(n)}(\boldsymbol{z}'|\boldsymbol{x})\right| \tag{24}$$

and for arbitrary $\varepsilon > 0$, define the set

$$A_n^\varepsilon := \left\{\boldsymbol{x}\in\mathbb{D}^{(n)} :\ M^{(n)}(\boldsymbol{x}) \le \varepsilon\right\}. \tag{25}$$

If A_n^ε were non-empty, then membership of the point $\boldsymbol{x}$ in A_n^ε implies

$$\left|\sup_{\boldsymbol{z}\in\mathbb{D}(\boldsymbol{x})} f^{(n)}(\boldsymbol{z}|\boldsymbol{x}) - \inf_{\boldsymbol{z}\in\mathbb{D}(\boldsymbol{x})} f^{(n)}(\boldsymbol{z}|\boldsymbol{x})\right| \le \varepsilon$$

and by virtue of (23), it then follows that

$$\left|f^{(n)}(\boldsymbol{z}|\boldsymbol{x}) - \frac{1}{\pi r_{min}^2}\right| \le \varepsilon, \quad \boldsymbol{z}\in\mathbb{D}(\boldsymbol{x}).$$

Given that ε can be selected arbitrarily small, this plausibility argument forms the basis for the statement that for sufficiently large n the conditional distribution of $\boldsymbol{X}^{(n)}$ given $[\boldsymbol{X}^{(n)} \in \mathbb{D}(\mathbf{X}_i)]$ can be approximated by a uniform distribution on $\mathbb{D}(\boldsymbol{x})$. This is formalized in the following results whose proof is provided in Appendix B.

Proposition 3 *For* all $\varepsilon > 0$, *we have* $\lim_{n\to\infty}\mathbf{P}\left[\boldsymbol{X}^{(n)}\in A_n^\varepsilon\right] = 1$.

7 Distribution of Link and Path Durations

We discuss how to approximate the distribution of link durations under the RWP mobility model without pause discussed in the two previous sections. To do so, we focus on two nodes, denoted by $n1$ and $n2$, that become neighbors at some time $t \ge 0$, and find the distribution of the link duration between them.

We assume that the radius of the disk a is sufficiently large $(a \gg r_{min})$ so that the conditional distribution discussed in the previous section can be approximated by a uniform distribution. Without loss of generality we assume $a = 1$ and scale other parameters accordingly. [6] This also implies that the average distance between two consecutive random waypoints selected by a node, is much larger than the transmission range r_{min}. Therefore, in most cases when two nodes become neighbors, with a high probability, neither of these two nodes will reach the next random waypoint before the link between them is torn down after they move out of the transmission range of each other. In other words, the average travel time of a node between two consecutive random waypoints selected by the node is much larger than the average link duration between two nodes. Hence, for simplicity of analysis we assume that neither node reaches its next random waypoint while they are neighbors, and truncate the link duration to model the arrival of the nodes at the random waypoints.

For the purpose of computing the distribution of link duration, rather than modeling the mobility of both nodes explicitly, we only model the net effects of mobility between the nodes by pretending that node $n1$ is fixed and modeling the relative motion of node $n2$ with respect to $n1$.

Denote the (relative) speed of node $n2$ with respect to node $n1$ by S. Then, the CDF of the link duration U, conditional on the relative speed S, can be approximated as

$$\begin{aligned}\mathbf{P}\left[U \leq d \mid S = s\right] &= \lim_{\varepsilon \downarrow 0} \mathbf{P}\left[U \leq d \mid s < S \leq s + \varepsilon\right] \\ &\approx g(d \cdot s) \end{aligned} \tag{26}$$

with

$$g(t) := \begin{cases} \left(1 - \sqrt{1 - \left(\frac{t}{2r_{min}}\right)^2}\right) \cdot u(t) & \text{if } t \leq 2r_{min} \\ 1 & \text{if } t > 2r_{min} \end{cases}$$

where $u(\cdot)$ is a unit step function. The derivation of (26) is provided in Appendix C. Therefore, if the distribution H of relative speed S is known, the CDF of the link duration U can be approximated using (26), and we obtain

$$\mathbf{P}\left[U \leq d\right] = \int_s \mathbf{P}\left[U \leq d \mid S = s\right] dH(s) \approx \int_s g(d \cdot s) dH(s) \,. \tag{27}$$

Let $\boldsymbol{V}^{(1)}$ (resp. $\boldsymbol{V}^{(2)}$) represent the velocity of node $n1$ (resp. $n2$). Since the mobility of a node is independent of that of the others, the relative motion of node $n2$ with respect to node $n1$ is simply the difference $\boldsymbol{V} = \boldsymbol{V}^{(2)} - \boldsymbol{V}^{(1)}$, as shown in Fig. 4.

[6] Note that fixing the disk radius and reducing the transmission range r_{min} is equivalent to fixing the transmission range first and allowing the disk radius to increase appropriately

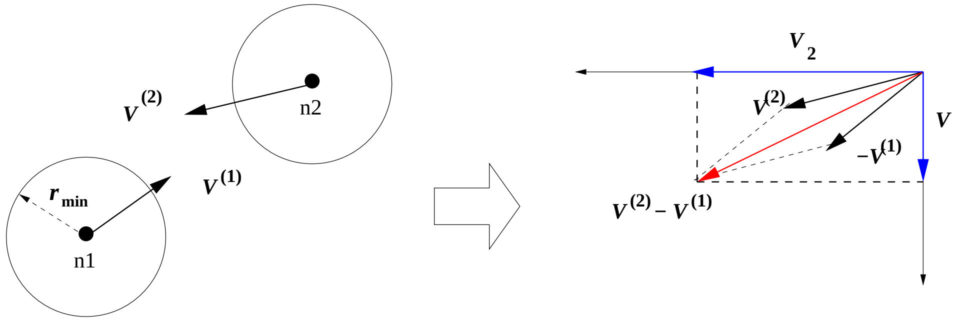

Fig. 4. Relative motion of $n2$ with respect to $n1$.

For simplicity of analysis, assume that the angle Θ' between $\boldsymbol{V}^{(2)}$ and $-\boldsymbol{V}^{(1)}$ is uniformly distributed in [0, 2π). Numerical examples obtained using ns-2 simulation in Section 8 show that this assumption introduces only a negligible amount of discrepancy in link duration distribution. Letting $S^{(i)} = \left\|\boldsymbol{V}^{(i)}\right\|$, we obtain the relative speed S between the nodes as

$$S = \sqrt{(S^{(1)} + S^{(2)} \cdot \cos\Theta')^2 + (S^{(2)} \cdot \sin\Theta')^2}\,,$$

and

$$\mathbf{P}\left[S \leq s\right] = \mathbf{P}\left[(S^{(1)} + S^{(2)} \cdot \cos\Theta^{'})^2 + (S^{(2)} \cdot \sin\Theta^{'})^2 \leq s^2\right], \quad s \geq 0 \tag{28}$$

Therefore, if we know the (stationary) distribution of $S^{(i)}$, we can numerically compute the CDF of S from (28).

If the speed is selected from the interval $[S_\star, S^\star]$, the PDF of the stationary distribution of the speed $S^{(i)}$ of node i is given by (16), and the CDF H of S can now be evaluated numerically via (28) and (16).

Once the CDF H becomes available, the CDF G of the link duration U can be calculated using (27), and the CDF F of the link excess life can be obtained from (6). The PDF of path duration with h hops is given by

$$f_{Z^{(n)}}(x) = \frac{h}{m(G)}(1 - F(x))^{h-1}(1 - G(x)), \quad x \geq 0\,. \tag{29}$$

In the next section we compare the numbers we obtain using this model against the simulation results obtained using ns-2 simulator.

for our purposes.

# of links	20,096	# of 1 hop paths	1,226
# of 2 hop paths	1,420	# of 3 hop paths	1,968
# of 4 hop paths	2,200	# of 5 hop paths	2,268
# of 6 hop paths	2,041	# of 7 hop paths	1,703

Table 1
Simulation statistics with $S_\star = 1$ m/s and $S^\star = 30$ m/s.

8 NS-2 Simulation Results

We now turn to validating the results of Section 4 by means of simulation results under the RWP mobility model without pause. The simulation results are obtained using the ns-2 simulator.

The simulation is run on a rectangular region of 2 km $\times$ 2 km. [7] There are 200 nodes moving across this region, and the transmission range of these nodes is fixed at 250 m. When a node selects the next random waypoint, it is selected according to a uniform distribution on the rectangular region. A node moves along a straight line connecting two consecutive random waypoints without a pause. Each simulation run lasts for 1,200 seconds, but we only look at the last 800 seconds in order to reduce the effects of the transient period. We take the average of 5 runs.

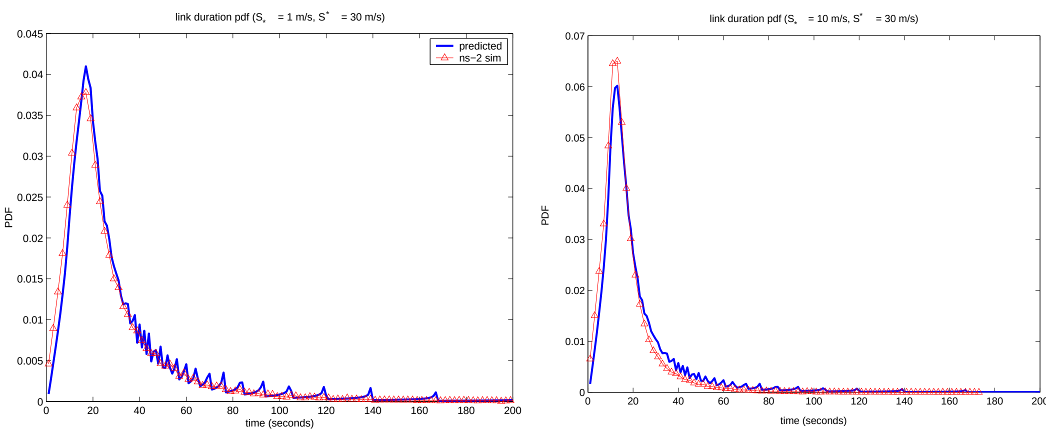

(a) (b)

Fig. 5. PDF of link duration. (a) $S_\star = 1$ m/s, $S^\star = 30$ m/s, (b) $S_\star = 10$ m/s, $S^\star = 30$ m/s.

We record the setup and teardown times of all the links that are established between any two nodes throughout the simulation and compute the empirical distribution of the durations of the links that are set up over the period of [400, 1200] seconds. The number of link statistics collected for the case with $[S_\star, S^\star] = [1, 30]$ m/s is 20,096 (Table 1). The empirical distribution of link duration from the simulation and the

[7] As mentioned earlier, the results in Section 6 for disks can be extended to the case with rectangular regions.

distribution computed from (27) are plotted in Fig. 5. Small fluctuations in the predicted distribution are due to the finite number of points used in the calculations.

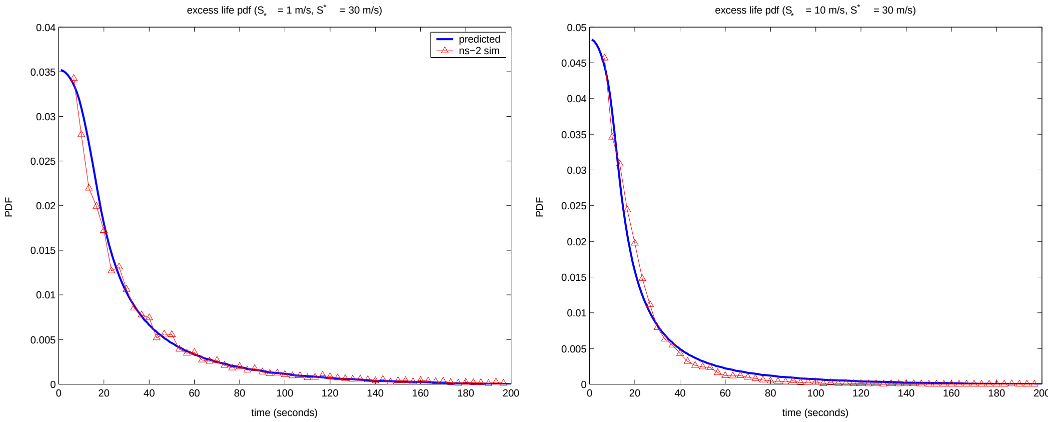

(a) (b)

Fig. 6. PDF of link excess life. (a) $S_\star = 1$ m/s, $S^\star = 30$ m/s, (b) $S_\star = 10$ m/s, $S^\star = 30$ m/s.

The PDF of a link excess life is plotted in Fig. 6 for both the ns-2 simulation and the model given by (6). As one can see, the PDFs computed from (27) and (6) match the empirical distributions very well, thus validating the accuracy of the model.

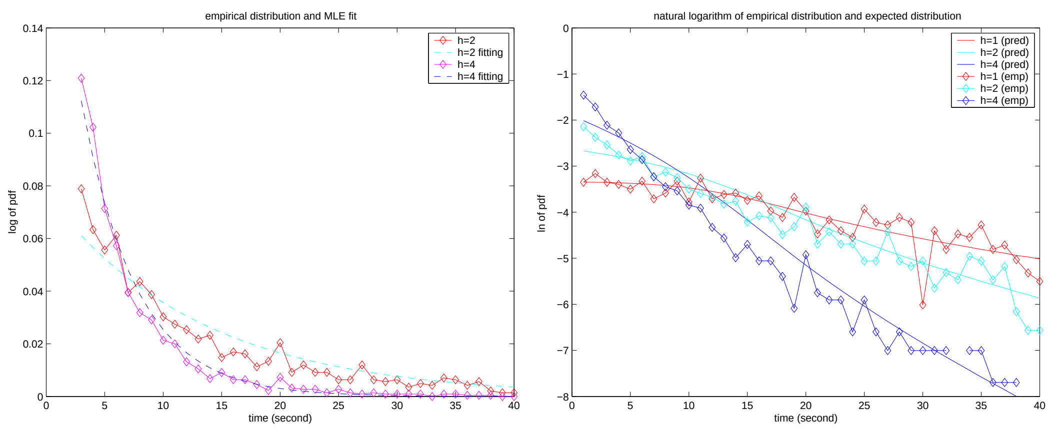

(a) (b)

Fig. 7. Exponential fitting of path duration distribution and comparison with predicted distribution ($S_\star = 1$ m/s and $S^\star = 30$ m/s). (a) Exponential fitting, (b) Plot of natural logarithm of empirical distribution and predicted distribution.

Similarly, as with the links, we record the time at which a path is set up and the time at which one of its links is broken, as well as the number of hops in the path. We plot the empirical PDF of path distribution for the paths with 2 and 4 hops in Fig. 7(a) and exponential fitting curves obtained using the MATLAB *expfit*($\cdot$) function. The maximum likelihood estimate parameters of the exponential distribution with hop counts $h = 2$ and $h = 4$ are 0.0770 and 0.2123, respectively. Although the measured distribution is a little noisy, the exponential fitting curve is seen to match the data well for $h = 4$, validating our claim in Theorem 2 that as the number of hops increases, the distribution of path duration can be well approximated by an exponential distribution. Our numerical results are consistent with the observations made in [16] that when the number of hops is larger than 3-4, the distribution closely resembles an exponential distribution.

Fig. 7(b) plots the natural logarithm of the empirical PDF of path duration and that of the predicted distribution from (29) (under the independence assumption) for hop counts $h =$ 1, 2, and 4. Despite the noise in the measurement and limited number of statistics collected, the simulation data follow the plot of the predicted distributions fairly closely, further validating the accuracy of our model.

9 Correlation of Link Excess Lives

In Section 4 we assumed that the stationary reachability processes $\{\xi_{ij}(t),\ t \geq 0\}$ are mutually independent, so that the excess lives of the links along a path are mutually independent. However, this assumption does not hold in general. We now take a closer look at this independence assumption of the excess lives of the links and attempt to provide some justification for it.

Observe that if two links along a path are separated by at least one other intermediary link, since no nodes are shared by the links, the excess lives of these links are expected to be at most weakly dependent, if not independent. However, two neighboring links share a node. In the example shown in Fig. 8, node $n2$ is shared by links $(n1, n2)$ and $(n2, n3)$. Since the excess lives of these two links depend on the mobility of node $n2$, the independence assumption is clearly not true in general in this case, and calls for a careful study.

Strictly speaking, the independence assumption does not hold between two neighboring links. However, we first demonstrate that the correlation coefficient between the excess lives of two neighboring links, which is a measure of dependency between them, is nonetheless rather small. Using the ns-2 simulation results, we will validate the statement that indeed the dependency between two neighboring links is weak, and two links separated by one or more links exhibit very little dependency, if any.

We adopt the model outlined in Section 5 and describe how we can approximate the correlation coefficient of the two neighboring links along a path. Without loss of generality we assume that two neighboring links under consideration are given by $(n1, n2)$ and $(n2, n3)$, which we denote by ℓ_1 and ℓ_2, respectively. Here we assume that the underlying routing protocol does *not* attempt to optimize the selected path, and nodes $n1$ and $n3$ are uniformly distributed within the transmission range of node $n2$ at the time of path selection. A more efficient routing protocol should not

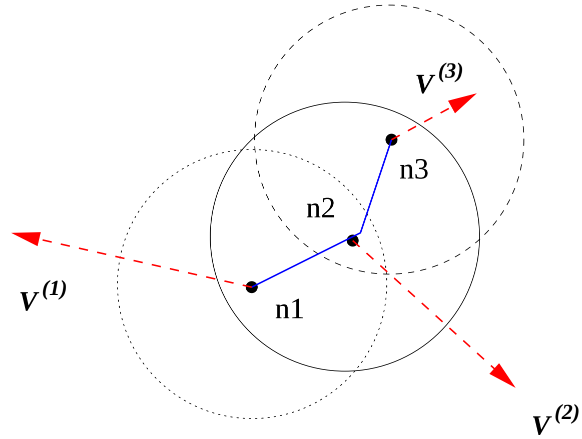

Fig. 8. Neighboring links.

select $n2$ as the next hop from $n1$ if $n3$ is within the transmission range of $n1$. However, due to the broadcast nature of a path request packet, node $n3$ may not receive the request message from node $n1$ correctly, and may reply only to the broadcast message from node $n2$.

Denote the excess life of link ℓ_i by X_i ($i = 1, 2$). The correlation coefficient of X_1 and X_2 is defined [18] to be

$$\rho_{X_1,X_2} = \frac{\mathbf{E}\left[X_1X_2\right] - \mathbf{E}\left[X_1\right]\mathbf{E}\left[X_2\right]}{\sqrt{Var(X_1)Var(X_2)}} = \frac{\mathbf{E}\left[X_1X_2\right] - \mathbf{E}\left[X_1\right]^2}{Var(X_1)}. \tag{30}$$

From the previous section we can compute the distribution F of the link excess life, and thus $\mathbf{E}\left[X_1\right]$ and $Var(X_1) = \mathbf{E}\left[(X_1)^2\right] - \mathbf{E}\left[X_1\right]^2$. The correlation $\mathbf{E}\left[X_1X_2\right]$ can be computed by conditioning on the speed $S^{(2)}$ of node $n2$. The details of the computation of the correlation $\mathbf{E}\left[X_1X_2\right]$ are provided in Appendix D.

If the node speed is chosen from the interval [1, 30] m/s, the correlation coefficient ρ of X_1 and X_2 calculated from our model (Eq. (D.4) in Appendix D) is approximately 0.0442. The correlation between the neighboring links is therefore rather weak, although they are not independent.

We also plot the empirical correlation coefficient obtained from the ns-2 simulation results as a function of the distance between links along a path. This is given in Fig. 9. The x-axis in the figure is the number of intermediate links between the links under consideration plus one; neighboring links have a distance of 1. The correlation coefficient is plotted on the y-axis. We see that the correlation between two links which are separated by at least one intermediate link between them is very weak, if they are not independent. Moreover, the dependency between neighboring links captured by the correlation coefficient in the plot is rather weak as well, which is consistent with our analysis in this section. Therefore, although our results indicate

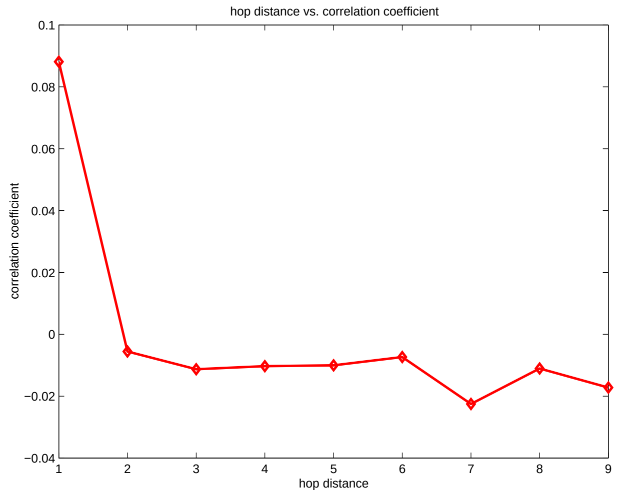

Fig. 9. Plot of hop vs. correlation coefficient (ns-2 simulation).

that the residual lives of links along a path may not be independent in general, both our analysis and numerical results suggest that any dependency that may exist is weak in the case of the RWP mobility model.

10 Conclusions

We have studied the distributional properties of path duration in multi-hop wireless networks. We have shown that, under certain conditions, the distribution of path duration (appropriately scaled) converges to an exponential distribution as the number of hops increases. The results were verified using a simple RWP mobility model. This allows us to compute the distribution of link duration given the distribution of speed of a node as well as the distributions of excess life and path duration.

The analysis was carried out under the assumption that the link durations are mutually independent. Although this may not be strictly true in general, we have shown in the case of RWP mobility model that the correlation of the excess lives of two neighboring links along a path is rather weak. Furthermore, even when link excess lives are dependent, we suspect that under certain dependence conditions, the distributional convergence established in this paper will continue to hold. We are currently investigating the correlation structure of link durations to understand the implications of link duration dependence on the performance of on-demand routing protocols and on the distributional properties of path duration.

References

[1] C. Bettstetter and C. Wagner, “The spatial node distribution of the random waypoint mobility model,” in Proceedings of German Workshop on Mobile Ad Hoc Networks (WMAN), Ulm (Germany), March 2002.

[2] J. Chang and L. Tassiulas, “Energy Conserving Routing in Wireless Ad-hoc Networks,” in Proceedings of IEEE Infocom, March 2000.

[3] T. L. Fine, *Probability and Probabilistic Reasoning for Electrical Engineering*, Pearson Prentice Hall, Upper Saddle River (NJ), 2005.

[4] J. Galambos, *The Asymptotic Theory of Extreme Order Statistics*, John Wiley & Sons, New York (NY), 1978.

[5] M. Grossglauser and D. Tse “Mobility Increases the Capacity of Ad Hoc Wireless Networks,” *IEEE/ACM Transactions on Networking*, Vol. 10(4), pp. 477-486, August 2002.

[6] P. Gupta and P. R. Kumar, “The capacity of wireless networks,” *IEEE Transactions on Information Theory* **IT-46** (2000), pp. 388-404.

[7] Y. Han, R. J. La, and A. M. Makowski, “Distribution of path durations in mobile ad-hoc networks – Palm’s Theorem at work,” in Proceedings of the ITC Specialist Seminar on Performance Evaluation of Wireless and Mobile Systems, Antwerp (Belgium), August 2004.

[8] Y. Han, and R. J. La, “Distribution of path durations in mobile ad-hoc networks with dependent link durations,” *in preparation.*

[9] D. P. Heyman and M. J. Sobel, *Stochastic Models in Operations Research, Volume I*, McGraw-Hill, New York, New York, 1982.

[10] D. B. Johnson, and D. A. Maltz, “Dynamic source routing in ad hoc wireless networks,” *Mobile Computing*, pp. 153-181, 1996.

[11] J.-Y. Le Boudec, “Understanding the simulation of mobility models with Palm calculus,” *available at http://icapeople.epfl.ch/leboudec*

[12] W. Navidi and T. Camp, “Stationary distributions of the random waypoint mobility model,” *IEEE Transactions on Mobile Computing* **ITMMC-3** (2004), pp. 99-108.

[13] C. E. Perkins, *Ad-hoc Networking,* Addison-Wesley Longman, Incorporated, 2000.

[14] S. Ramanathan and E. Lloyd, “Scheduling Algorithms for Multi-hop Radio Networks,” *IEEE/ACM Transactions on Networking*, Vol. 1(2), pp. 166-177, April 1993.

[15] V. Rodoplu and T. Meng “Minimum Energy Mobile Wireless Networks,” *IEEE Journal on Selected Areas in Communications*, Vol. 17(8), pp. 1333-1344, August 1999.

[16] N. Sadagopan, F. Bai, B. Krishnamachari, and A. Helmy, "PATHS: Analysis of path Duration statistics and the impact on reactive MANET routing protocols," in Proceedings of ACM MobiHoc, Annapolis (MD), June, 2003.

[17] C.-K. Toh, *Ad-hoc Mobile Wireless Networks: Protocols and Systems*, Prentice Hall PTR, 2001.

[18] R. D. Yates and D. J. Goodman, *Probability and Stochastic Processes*, Wiley, 1999.

A Appendix I
Reachability Processes Based on Physical Layer Models

As mentioned in Section 2, the reachability processes can be defined based on the physical channel characteristics.

In the simplest form, one can assume that node i can decode the packets from node j if and only if the received signal power exceeds some threshold $\Gamma > 0$ [2,15]. If P_i is the maximum transmission power of node i, this implies that the reachability process between nodes i and j is given by (3) with $\Psi_i(t) = 1$ as the numerators give the largest achievable received signal power at the nodes.

Similarly, if one assumes that packets can be successfully decoded if the achieved SINR exceeds the threshold Γ [6,5], then the reachability process between nodes i and j is again determined through by (3) with

$$\Psi_i(t) = W_i + \sum_{k \in TX(t) \setminus \{j\}} P_k(t) \cdot F_{ki}(t) \ , \tag{A.1}$$

where W_i is the noise variance at node i, $TX(t)$ is the set of transmitters at time t and $P_k(t)$ denotes the transmission power of node k. The right hand side of (A.1) represents the sum of noise power and the interference at node i at time t. This implies that nodes i and j have connectivity if and only if the achieved SINR value using the maximum transmission power exceeds Γ in both directions.

B Appendix II
A Proof of Proposition 3

Let $\{\beta_n, \ n = 1, \ldots\}$ be a sequence of positive constants in $(0, 1)$ such that (i) $\lim_{n\to\infty} \beta_n = 0$, and (ii) $\lim_{n\to\infty} \beta_n \cdot a_n = \infty$ so that (iii) $\lim_{n\to\infty}(1-\beta_n)\cdot a_n = \infty$. If $\mathbb{D}_n^\star$ denotes the disk centered at the origin with radius $(1 - \beta_n)a_n$, then an easy calculation based on (17) shows that $\mathbf{P}\left[\boldsymbol{X}^{(n)} \in \mathbb{D}_n^\star\right] = (1 - \beta_n)^2(2 - (1 - \beta_n)^2)$, whence

$$\lim_{n\to\infty} \mathbf{P}\left[\boldsymbol{X}^{(n)} \in \mathbb{D}_n^\star\right] = 1. \tag{B.1}$$

We shall show shortly that

$$\lim_{n\to\infty} \sup_{\boldsymbol{x}\in\mathbb{D}_n^\star} M^{(n)}(\boldsymbol{x}) = 0. \tag{B.2}$$

In that case, for all $\varepsilon > 0$, there exists a finite integer $n^\star = n^\star(\varepsilon)$ such that

$$M^{(n)}(\boldsymbol{x}) \leq \varepsilon, \quad n = n^\star, n^\star + 1, \ldots \tag{B.3}$$

for *all* $\boldsymbol{x}$ in $\mathbb{D}_n^\star$. As a result, the set A_n^ε is not empty for large enough n since $\mathbb{D}_n^\star \subseteq A_n^\varepsilon$, and the conclusion of Proposition 3 immediately follows from (B.1).

In order to show (B.2), fix $n = 1, 2, \ldots$ large enough so that $(1-\beta_n)\cdot a_n + r_{min} < a_n$; this is possible by (ii) and (iii). Then, note that for $\boldsymbol{x}$ in $\mathbb{D}_n^\star$, the disk $\mathbb{D}(\boldsymbol{x})$ is now completely contained in $\mathbb{D}^{(n)}$. Thus, by the definition (24) of $M^{(n)}(\boldsymbol{x})$, we get

$$M^{(n)}(\boldsymbol{x}) = \mathbf{P}\left[\boldsymbol{X}^{(n)} \in \mathbb{D}(\boldsymbol{x})\right]^{-1} \cdot \sup_{\boldsymbol{z},\boldsymbol{z}'\in\mathbb{D}(\boldsymbol{x})} \left| f_{a_n}(\boldsymbol{z}) - f_{a_n}(\boldsymbol{z}')\right| \tag{B.4}$$

as we make use of (22). The approximation (19) readily yields

$$M^{(n)}(\boldsymbol{x}) = \frac{1}{C_n(\boldsymbol{x})} \cdot \sup_{\boldsymbol{z},\boldsymbol{z}'\in\mathbb{D}(\boldsymbol{x})} \left| ||\boldsymbol{z}||^2 - ||\boldsymbol{z}'||^2 \right| \tag{B.5}$$

with

$$C_n(\boldsymbol{x}) := \frac{\pi a_n^4}{2} \cdot \mathbf{P}\left[\boldsymbol{X}^{(n)} \in \mathbb{D}(\boldsymbol{x})\right].$$

Substituting the relation

$$\mathbf{P}\left[\boldsymbol{X}^{(n)} \in \mathbb{D}(\boldsymbol{x})\right] = \frac{2}{\pi a_n^2} \int_{\mathbb{D}(\boldsymbol{x})} \left(1 - \frac{||\boldsymbol{z}||^2}{a_n^2}\right) d\boldsymbol{z}$$

into the expression for $C_n(\boldsymbol{x})$, we find

$$C_n(\boldsymbol{x}) = a_n^2 \int_{\mathbb{D}(\boldsymbol{x})} \left(1 - \frac{||\boldsymbol{z}||^2}{a_n^2}\right) d\boldsymbol{z}$$

$$= \pi a_n^2 r_{min}^2 - \int\limits_{\mathbb{D}(\boldsymbol{x})} ||\boldsymbol{z}||^2 \, d\boldsymbol{z}$$

$$\geq \pi r_{min}^2 \cdot \left(a_n^2 - \max_{\boldsymbol{z} \in \mathbb{D}(\boldsymbol{x})} ||\boldsymbol{z}||^2 \right). \tag{B.6}$$

Direct geometric arguments show that

$$\sup_{\boldsymbol{z}, \boldsymbol{z}' \in \mathbb{D}(\boldsymbol{x})} \left| ||\boldsymbol{z}||^2 - ||\boldsymbol{z}'||^2 \right| \leq 4 r_{min} \, ||\boldsymbol{x}|| \tag{B.7}$$

and

$$\max_{\boldsymbol{z} \in \mathbb{D}(\boldsymbol{x})} ||\boldsymbol{z}||^2 = \left(1 + \frac{r_{min}}{||\boldsymbol{x}||} \right)^2 ||\boldsymbol{x}||^2 = \left(||\boldsymbol{x}|| + r_{min} \right)^2. \tag{B.8}$$

Thus, combining the facts (B.7) and (B.8), we conclude from (B.5) that

$$M^{(n)}(\boldsymbol{x}) \leq \frac{4}{\pi r_{min}} \cdot \frac{||\boldsymbol{x}||}{a_n^2 - \left(||\boldsymbol{x}|| + r_{min} \right)^2}, \quad \boldsymbol{x} \in \mathbb{D}_n^\star \tag{B.9}$$

Elementary calculus now shows that the bound in (B.9) achieves its maximum over the set $\mathbb{D}_n^\star$ when $||\boldsymbol{x}|| = (1 - \beta_n) a_n$. Thus,

$$\sup_{\boldsymbol{x} \in \mathbb{D}_n^\star} M^{(n)}(\boldsymbol{x}) \leq \frac{4}{\pi r_{min}} \cdot \frac{(1 - \beta_n) a_n}{a_n^2 - \left((1 - \beta_n) a_n + r_{min} \right)^2} \tag{B.10}$$

and the desired conclusion (B.2) follows.

C Appendix III
Derivation of Approximation in (26)

Consider two nodes $n1$ and $n2$ that become neighbors at some time $t \geq 0$, as shown in Fig. C.1. Let ϕ denote the distance between $n1$ and $n2$ when they are closest to each other. The location of node $n2$ when the distance between them is ϕ, is denoted by x as shown in Fig. C.1. We draw a reference line that is perpendicular to the arrow from $n1$ to x and goes through $n1$; this is shown as a long solid line in Fig. C.1. Note that the relative motion of node $n2$ with respect to node $n1$ is parallel to the reference line. Also, the relative motion of node $n2$ is parallel to this reference line and they become neighbors at some point (before the angle between the reference line and the arrow from $n1$ to $n2$ becomes $\frac{\pi}{2}$). Thus, under the steady

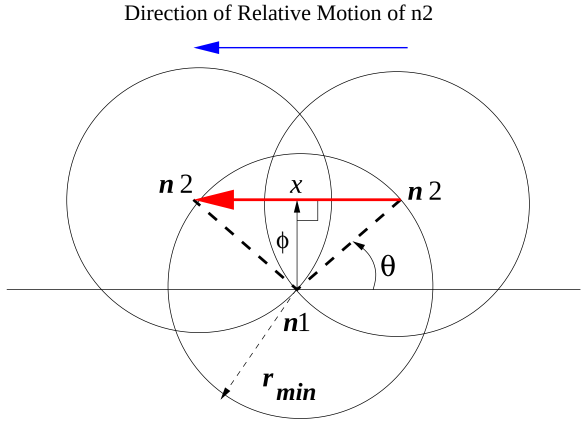

Fig. C.1. Link duration.

state assumption along with the assumption $r_{min} \ll 1$, the minimum distance ϕ is approximately uniformly distributed on the interval $[0, r_{min})$ from Proposition 3.

Given the (relative) speed of node $n2$, denoted by S, and the angle of the arrow from node $n1$ to node $n2$ with the reference line when $n2$ first comes within the transmission range of $n1$, denoted by Θ in Fig. C.1, the duration of the link between these two nodes is given by

$$U(S, \Theta) = \frac{2r_{min} \cos\Theta}{S} \ . \tag{C.1}$$

Therefore, from the independence of mobility of nodes, we can approximate the CDF of link duration U conditional on the relative speed S as follows: Using (C.1), we get

$$\begin{aligned}
\mathbf{P}\left[U \leq d \mid S = s\right] &= \mathbf{P}\left[\frac{2r_{min}\cos\Theta}{s} \leq d\right] \\
&= \mathbf{P}\left[\cos\Theta \leq \frac{d \cdot s}{2r_{min}}\right] \\
&= \mathbf{P}\left[\sin\Theta \geq \sqrt{1 - \left(\frac{d \cdot s}{2r_{min}}\right)^2}\right] \\
&\approx \begin{cases} \left(1 - \sqrt{1 - \left(\frac{d \cdot s}{2r_{min}}\right)^2}\right) \cdot u(d) & \text{if } d \leq \frac{2r_{min}}{s} \\ 1 & \text{if } d > \frac{2r_{min}}{s} \end{cases}
\end{aligned}$$

where the last approximation follows from the fact that $r_{min} \cdot \sin\Theta = \phi$ so that $\sin\Theta$ is approximately uniformly distributed in $[0, 1)$ as explained earlier.

D Appendix IV Calculation of Correlation $\mathbf{E}[X_1 X_2]$

We explain how the correlation $\mathbf{E}[X_1X_2]$ in (30) can be computed in the RWP mobility model under consideration. By conditioning on the speed $S^{(2)}$ of node $n2$, we have

$$\mathbf{E}[X_1X_2] = \mathbf{E}\left[\mathbf{E}\left[X_1X_2 \mid S^{(2)}\right]\right] = \int_s \mathbf{E}\left[X_1X_2 \mid S^{(2)} = s\right] dQ(s)$$

where Q is the distribution of $S^{(2)}$ at steady state. If the node speed is selected from the interval $[S_\star, S^\star]$, then (16) yields

$$\mathbf{E}[X_1X_2] = \left(\ln\left(\frac{S^\star}{S_\star}\right)\right)^{-1} \cdot \int_{S_\star}^{S^\star} \mathbf{E}\left[X_1X_2 \mid S^{(2)} = s\right] \frac{ds}{s}.$$

We now describe how to compute the conditional expected value $\mathbf{E}\left[X_1X_2 \mid S^{(2)} = s\right]$. This requires computing the conditional distribution of the relative speed between $n2$ and its neighbors given the value of $S^{(2)}$, which is different from the a priori distribution of the relative speed used in Section 7. However, the calculation of this conditional distribution can be carried out in a similar manner.

Without loss of generality, we take the link $\ell_1 = (n1, n2)$ to compute the link duration distribution conditional on the value of $S^{(2)}$. Suppose that the mobility of node $n1$ (resp. $n2$) is represented by $\boldsymbol{V}^{(1)}$ (resp. $\boldsymbol{V}^{(2)}$) as before and assume that the angle Θ' between $\boldsymbol{V}^{(1)}$ and $-\boldsymbol{V}^{(2)}$ is uniformly distributed in $[0,\ 2\pi)$. With a little abuse of notation, the CDF of the relative speed S of node $n1$ with respect to node $n2$ conditional on $S^{(2)}$ is given by

$$\begin{aligned} H_{s_2}(s) &= \mathbf{P}\left[S \le s \mid S^{(2)} = s_2\right] \\ &= \mathbf{P}\left[(S^{(1)} \cdot \cos\Theta' + s_2)^2 + (S^{(1)} \cdot \sin\Theta')^2 \le s^2\right] \end{aligned} \tag{D.1}$$

where $S^{(1)} = \left\|\boldsymbol{V}^{(1)}\right\|$. The conditional distribution $H_{s_2}(s)$ of the relative speed in (D.1) can be used to compute the conditional distribution of link duration from

$$\begin{aligned} G_{s_2}(d) &= \mathbf{P}\left[U \le d \mid S^{(2)} = s_2\right] \\ &= \int_s \mathbf{P}\left[U \le d \mid S^{(2)} = s_2, S = s\right] dH_{s_2}(s) \\ &= \int_s \mathbf{P}\left[U \le d \mid S = s\right] dH_{s_2}(s) \end{aligned} \tag{D.2}$$

Using (D.2), the conditional link excess life distribution given $S^{(2)} = s_2$ can be computed according to

$$
\begin{aligned}
F_{s_2}(x) &= F(x \mid S^{(2)} = s_2) \\
&= \begin{cases} \frac{1}{m(G_{s_2})} \int_0^x (1 - G_{s_2}(y))\, dy & \text{if } x > 0 \\ 0 & \text{if } x \leq 0 \end{cases}
\end{aligned} \tag{D.3}
$$

where $m(G_{s_2})$ is the mean of G_{s_2}.

Since X_1 and X_2 are conditionally independent given the speed $S^{(2)}$ of node $n2$, the correlation $\mathbf{E}[X_1 X_2]$ can be computed using (D.3) as

$$
\begin{aligned}
\mathbf{E}[X_1 X_2] &= \mathbf{E}\left[\mathbf{E}\left[X_1 X_2 \mid S^{(2)}\right]\right] \\
&= \int_{s_2} \mathbf{E}\left[X_1 X_2 \mid S^{(2)} = s_2\right] dQ(s_2) \\
&= \int_{s_2} \left(\int_{x_1} x_1 dF_{s_2}(x_1) \int_{x_2} x_2 dF_{s_2}(x_2) \right) dQ(s_2)\ .
\end{aligned} \tag{D.4}
$$